Magnetic properties of first-row element-doped ZnS semiconductors: a density functional theory investigation

Run Long, Niall J. English

The SEC Strategic Research Cluster and the Centre for Synthesis and Chemical Biology, Conway Institute of Biomolecular and Biomedical Research, School of Chemical and Bioprocess Engineering, University College Dublin, Belfield, Dublin 4, Ireland

Based on first-principles calculations, we have investigated the magnetic properties of the first-row element-doped ZnS semiconductors. Calculations reveal that Be, B, and C dopants can induce **magnetic**, while N cannot lead to spin polarization in ZnS. A possible explanation was rationalized from the elements' electronegativity and interaction between dopant atoms and host atoms. The total magnetic moments are 2.00, 3.16, and 2.38 μ_B per $2 \times 2 \times 2$ supercell for Be, B, and C doping, respectively, and ferromagnetic coupling is generally observed in these cases. The ferromagnetism of Be-, B-, and C-doped ZnS can be explained by hole-mediated ***s*-*p* or** *p*-*p* interactions' coupling mechanisms**. However, the clustering effect was found to be in Be-, B-, and C-doped ZnS but the degree is more obvious in the former two cases than in latter case.** Analysis revealed that C-doped ZnS displays better potential ferromagnetic behavior than Be- and B-doped ZnS due to its half-metallic characteristic.

Keywords: ZnS, doped, ferromagnetic coupling

1. Introduction

Dilulted magnetic semiconductors (DMSs) have attracted intense interest due to their potential applications in spintronics devices [1]. To date, most of the attention on DMSs has been focused on transition metal (TM)-doped semiconductors, such as GaN and ZnO [2-4]. Typically, the Curie temperatures of such systems are below room temperature, meaning that they are difficult to use in practice. Recently, room-temperature ferromagnetism was reported in TM-doped DMSs, but it was difficult to avoid the presence of TM clustering or secondary phases [5]. In addition, for group II-VI semiconductors, it is difficult to dope such materials effectively to realize p- or n-type devices due to their intrinsic band gap. A possible way to overcome this drawback is to use non-metal elements to substitute TM magnetic elements to dope such semiconductors. In fact, there are many papers which have reported that non-metal elements induce magnetic behavior both experimentally and theoretically [6-13]. It has been demonstrated that room-temperature ferromagnetism can be achieved in ZnO by doping with C [6]. Subsequently, it has been reported that stable ferromagnetism is extant in C-doped CdS and C-ZnS [7, 8]. Other non-metal elements, such as Be, B and N, can also lead to ferromagnetism in AlN and ZnO, respectively [9]. Therefore it is possible that such non-metal elements could also induce ferromagnetic coupling in ZnS. However, only Fan et al. [8] have reported electronic structure and magnetic properties of C anion-doped ZnS; a detailed theoretical investigation and comparison of Be, B and N-doped ZnS has not been reported to date, to the best of our knowledge.

In the present study, we have **employed** first-principles calculations to study the magnetism and electronic structure of X (Be, B, C, N)-doped ZnS systematically. Calculations indicate that doping by Be, B, and C atoms in ZnS could induce ferromagnetic coupling in ZnS through hole-mediated interactions. The magnetic moments were 2.00, 3.16 and 2.38 μ_B for Be-, B- and C-doped 64-atom ZnS containing one substitutional dopant atom. However, the N dopant did not result in spin polarization in N-doped ZnS. Consideration of the elements' electronegativity and bonding characteristics can explain the different behavior in doped systems for B, Be, C, and N. The electronic structures show that Be-doped ZnS induce deep acceptor levels inside the band gap, while B-doped ZnS is a p-type semiconductor and C-doped ZnS is a p-type half-metallic ferromagnetic semiconductor. **The *p*-*d* exchanges-like *p*-*p* coupling (*s*-*p* coupling for Be-doped ZnS)**, were found to be responsible for the ferromagnetic behavior.

2. Methodology

The spin-polarized calculations were performed using the projector augmented wave (PAW) pseudopotentials as implemented in the Vienna ab initio Simulation Package (VASP) code [14, 15]. The Perdew and Wang parameterization [16] of the generalized gradient approximation (GGA) [17] was adopted for the exchange-correlation potential. The electronic wave function was expanded in plane waves up to a cutoff energy of 400 eV and a Monkhorst–Pack *k*-point mesh [18] of 4 × 4 × 4 was used for geometry optimization and electronic property calculations. **Both**

the atomic positions and cell parameters were optimized until the residual forces were below 0.01 eV/Å. The ZnS was modeled by a 2×2×2 64-atom **zinc** blende structure ZnS supercell and doped systems were constructed with one or two dopant atoms to substitute host S atoms. The optimized lattice parameter for pure ZnS was 5.446 Å, in good agreement with an experimental value of 5.41 Å [19], indicating that our methodology is reasonable.

3. Results and discussions

Firstly, we show the structural and energy results for different doping systems. In this case, one dopant atom was substituted for an S atom in the 64-atom supercell (cf. Figure 1, site 1); the calculated results are listed in Table 1. After geometry relaxation, the relaxed X-Zn (X = Be, B, C, N) bond length was 2.354, 2.209, 2.056, and 1.980 Å, respectively, which are all less than that of the optimal S-Zn bond length of 2.358 Å. The local structure around the dopant atoms was slightly suppressed with the Zn atoms **close** to the dopant atom.

To investigate the stability of doped ZnS, the defect formation energy E_{form} was calculated according to the following formula **[7, 8, 20]**

$$E_{form} = E(doped) - E(pure) + n(\mu_S - \mu_X) \quad (1)$$

where $E(doped)$ and $E(pure)$ are the total energy of the ZnS supercell with and without the X dopants. μ_X is the chemical potential for the X dopants (X=Be, B, C, or N) and μ_S is the chemical potential for S host atom, which depends on the material growth conditions and satisfies boundary conditions. **n is the number of S atoms**

replaced by X dopants. We employed the same method as by Fan et al. [8] to calculate the chemical potentials for host and dopant atoms (*i.e.*, the energies of an isolated S, Be, B, C, and N atom, respectively). The results are summarized in Table 1. It shows that the formation energies are **5.47**, **2.69**, **1.49**, and **1.33** eV, respectively. The smaller the formation energy, the easier the dopants' incorporation into the ZnS lattice; this indicates that C- and N-doped ZnS may be realized easily experimentally. Our calculated formation energy was **1.49** eV, which is **a bit larger than** 0.98 eV reported in previous work [8].

Calculations show that Be, B and C-doped ZnS materials favor spin-polarized (E_{sp}) states and its total energy is 187, 501, and 98 meV lower than that of nonspin-polarized (E_{nsp}) states ($\Delta E = E_{nsp}-E_{sp}$), respectively, as shown in Table 1; this indicates that the spin-polarized state is stable. However, there is an equivalent total energy between spin-polarized and nonspin-polarized calculations, suggesting that N cannot lead to spin splitting in N-doped ZnS; this was confirmed by subsequent electronic structure results (*vide infra*).

The calculated magnetic moments were 2.00, 3.16 and 2.38 μ_B for Be, B, and C doped-ZnS supercells, respectively. However, as stated previously, N doping did not lead to magnetic behavior. For Be-doped ZnS, the total magnetic moment (2.00 μ_B) per supercell arises mainly from Be atoms (0.57 μ_B per Be atom). Each nearest neighboring Zn atom contributed 0.23 μ_B, and each second-nearest neighboring S atom contributed 0.044 μ_B. For B-doped ZnS, the total magnetic moment (3.16 μ_B / B) per supercell is attributable mainly to the B atom itself (1.01 μ_B / B). Each nearest

neighboring Zn atom provided 0.32 μ_B, and each second-nearest S atom contributed 0.07μ_B. For C-doped ZnS, the total magnetic moment per supercell (2.38μ_B / C) was due principally to C atom (0.70μ_B/C), which is slightly larger than 2.00 μ_B per supercell reported by Fan et al. in C-doped ZnS [8]. Each nearest-neighboring Zn atom contributed 0.14 μ_B, and each second-nearest neighboring S atom contributed 0.082 μ_B. **It is well known that so many factors can influence magnetic moment value, such as the supercell volume, local structure and so on. Certainly, the supercell volume is 1274.43 Å^3 (not shown this value in Ref. [8]) and the difference of Zn-C bond length between us and Ref. [8] is 0.007 Å. These two reasons may account for the difference of total magnetic moment and local magnetic moment on C atom between us and Fan et al. [8].** In all of these doped systems, the magnetic moments are oriented in the same direction, indicating ferromagnetic coupling between the dopant (Be, B, C) and neighboring host atoms.

Figure 2 shows the calculated total density of states (DOS) and the projected DOS (PDOS) of ZnS with one S atom substituted by dopant atoms (Be, B, C and N) and one of the neighboring S and Zn atoms. The interaction between the atomic orbitals and the conduction band (CB) or valence band (VB) leads to the formation of **anti-bonding** and **bonding** states. In the case of N as the dopant, these bonding and anti-bonding states will reside in the **VB** and **CB, respectively**. The electronegativities are in the order Be (1.57) < B (2.04) < C (2.55) < S (2.58) < N (3.04) [**21**]. Since Be, B, and C are less electronegative than N, they therefore tend to interact less with the host semiconductor. Therefore the **bonding** or **anti-bonding**

states due to the interaction with the VB or CB cannot be pushed up or down into the CB or VB, and therefore stay in the gap. As shown in Figure 2, the **2s** orbitals of Be, **2p orbitals of** B, and C locate in the gap and are very small within the host CB and VB, indicating that they are bonded more weakly to Zn atoms than N, and therefore their **2s or** 2p orbitals are more localized. This leads to spin-polarization of their **2s or** 2p states, to reduce the Coulombic interaction energy and the total system energy to keep the system stable. On the other hand, N is more electronegative than S and interacts with the host atoms more strongly, which results in bonding and anti-bonding states giving a larger splitting while they still reside in the host bands. The above bond length also indicates that the interaction between dopant atoms and Zn atoms was in the order Be-Zn < B-Zn < C-Zn < N-Zn.

Figure 2 shows that all of Be, B, and C dopants change the DOS significantly near the Fermi level E_F and results in a significant spin polarization of the valence band (VB) but does not induce spin polarization of the conduction band (CB). Strong coupling between the **s orbitals** of Be, **p orbitals of** B, C and S atom and the d orbitals of Zn atoms near the Fermi level can be seen clearly. The d orbitals of Zn are hybridized with the **s or** p orbitals of the dopant and host S atom. The spin-up bands are fully occupied for B- and C-doped ZnS, while the spin-down bands are empty, leading to a significant spin-splitting. At the same time, the position of Fermi level in B-, and C-doped ZnS is different. In particular, E_F was between majority- and minority-spin states in B-doped ZnS and was in the VB tail in C-doped ZnS, indicating that the former system constitutes a good p-type ferromagnetic

semiconductor and the latter case a p-type half-metallic ferromagnetic semiconductor. This suggests that for these two cases, the charge carriers within the impurity bands are sufficiently mobile, which is not only beneficial for conductive behavior but also for the magnetic coupling. Furthermore, half-metallic character of C-doped ZnS can complete spin polarization (100%) at the Fermi level, which is important for spintronic applications [**22**]. On the other hand, E_F was pinned to the impurity states in the band gap of Be-doped ZnS, which implies that the extent of electronic localization is high, and that electrons cannot move freely. Hence, Be-doped ZnS possesses weak conductive behavior and does not facilitate magnetic interaction.

Based on the above analysis, we have selected C-doped ZnS as an example for analysis of its spin-density distribution. This is shown in Figure **3** (a), where the spin density in C-doped ZnS is localized mainly on the C atom and distributed slightly over its four nearest-neighboring Zn atoms and the twelve second nearest-neighboring S atoms. This indicates that magnetic orbital coupling extends to the second nearest-neighboring S atoms from the C dopant centres. Therefore, anions from the delocalized p orbitals contribute chiefly to the magnetic moment in C-doped ZnS.

To investigate the magnetic order, we investigated two dopant atoms substituted for two S atoms in the ZnS host semiconductor. Five possible and independent configurations of the two dopant atoms were considered, *i.e.*, Be (B, C)$_{0i}$ (i = 1~5), as shown in Figure 1. In each case, one dopant atom occupied position 0, and the other dopant atom was located at other host S atom positions (1~5). The energy difference between ferromagnetic (FM) and anti-ferromagnetic states (AFM) ($\Delta E = E(FM) -$

E(AFM)) for three doped configurations are summarized in Tables 2-4, respectively. Calculations indicated that there exists a FM state in Be-, B-, and C-doped ZnS semiconductors, suggesting that long-range ferromagnetic coupling exists between the three kinds of dopant atoms. Such large energy differences between FM and AFM states for the three doped FM systems (380, 751 and 121 meV in (0, 5), (0, 5) and (0, 4) configurations for Be, B and C-doping, respectively) suggest that room-temperature ferromagnetism for Be, B-, and C-doped ZnS is quite feasible. However, C-doped ZnS in different configurations are not always in the FM state in our calculations, which contrasts with Fan et al. [8] who reported that FM state is always ground state. Our energy results indicate that the existence or stability of FM, AFM, and para-feromagetic behavior may depend on the distance between two C dopant atoms. The same effect was observed in Be-doped ZnS. However, the nearest distance for the (0, 1) case of two dopant atoms exhibits the lowest formation energies and is over 1 and 0.57 eV lower than others in Be- and B-doped ZnS, respectively, indicating a clustering effect of Be and B. On the other hand, the formation energies of the (0, 1) **AFM** configuration is only **about 0.08** eV lower than the FM (0, 4) configuration in C-doped ZnS, indicating that the clustering effect is not obvious. This would suggest that C-doped ZnS displays the best potential ferromagnetic behavior among the three doped systems.

At this point, it is instructive to investigate the magnetic coupling between the two dopant atoms. Magnetic coupling was found to exist even if the separation distance was 9.355 Å for Be- and B-doped ZnS (the (0, 5) configuration) and by 7.638 Å for

C-doped ZnS (the (0, 4) case). However, both double- and super-exchange interactions cannot account for long-range magnetic order at low doping concentrations of a few percent. **The double-exchange occurs due to electron exchange via unoccupied band or impurity-related band of two adjacent dopants without spin reversal [23, 24]. The electron cloud should at least overlap each other. In our cases, the distance between two dopants is very large and the doping concentrations are very low simultaneously. It seems that double-exchange cannot be responsible for long-range FM coupling. Additionally, although the double-exchange via empty states in the conduction band may also contribute, this contribution is small in zinc blende host crystals because the hybridization between the impurity d-states and the s-states of the electrons near the bottom of conduction band is weak due to the symmetry selection rules [25, 26].** Hence, it is possible that ***p-d*** **exchanges-like** ***p-p*** **coupling (*s-p* coupling for Be-doped ZnS)** involving holes, are responsible for the observed long-range magnetic coupling, similar to N-doped ZnO [10]. For conciseness, we have selected C-doped ZnS as a representative system to discuss long-range magnetic coupling. Figure **3** (b) shows magnetic coupling between two C atoms. As can be seen, the nearest-neighbour anions between dopants mediate the magnetic coupling. Obviously, the charge carriers localized around the anions between the C atoms are polarized and that the spin orientations are parallel to each other. Consequently, these polarized charge carriers mediate the long-range ferromagnetic coupling between the dopant atoms. There are four valence electrons in a C ion, which has two less valence

electrons than an S ion. Replacement of S by C introduces more holes into the valence band. Hole-mediated ferromagnetism may be responsible for magnetic coupling. The strong *p-p* interaction leads to a stronger coupling between impurity and carrier spin orientations. Sufficiently large spin-polarized carriers are able to effectively mediate indirect long-range ferromagnetic coupling between the C dopants, as shown in Figure **3** (b). The spatially extended p states of the host and the impurity are able to extend the p-p interaction and spin alignment to longer range, and thus to cause long-range magnetic coupling between the impurities. Similar analysis may be applied to Be- and B-doped ZnS.

4. Conclusions

We have studied Be, B, C, and N anion-doped ZnS by means of density functional theory calculations. It has been shown that Be, B, and C impurities acquire magnetization, leading to a magnetic moment of 2.00, 3.16 and 2.38 μ_B per $2 \times 2 \times 2$ supercell, while N-doped ZnS displays no magnetic behavior. The lower Be, B, and C electronegativities vis-à-vis S lead to weaker interactions between dopants and host atoms, and serve to keep the dopants' **2s or** 2p states within the band gap. Conversely, the larger N electronegativity in comparison to S leads to a stronger interaction between N and host atoms which results in the 2p states residing in the host bands. The magnetic moments of Be, B, and C and its neighboring Zn and S atoms are parallel. Based on the calculated results that impurity bands are located within the band gap and the Fermi level crosses the impurities, long-rang ferromagnetic coupling

between two dopant atoms has been attributed to hole-mediated *p*-*p* coupling **(*s*-*p* coupling for Be-doped ZnS)** interactions. **The clustering effect was found in three doped systems although it's not obvious in C-doped ZnS.** Considering its lower formation energy, room-temperature ferromagnetism and half-metallic characteristic of C-doped ZnS may be more easily achievable with respect to Be- and B-doped ZnS.

Acknowledgements

This work was supported by the Irish Research Council for Science, Engineering and Technology (IRCSET). The authors thank the Irish Centre for High End Computing and Science Foundation Ireland for the provision of computational resources.

Reference

1 H. Ohno, Science **281**, 951 (1998).

2 C. Liu, F. Yun, and H. Morko, J. Mater. Sci.: Mater. Electron. **16**, 555 (2005).

3 H. Munekata, H. Ohno, S. von Molnar, Armin Segmüller, L. L. Chang, and L. Esaki, Phys. Rev. Lett. **6**3, 1849 (1989).

4 M. H. F. Sluiter, Y. Kawazoe, P. Sharma, A. Inoue, A. R. Raju, C. Rout, and U. V. Waghmare, Phys. Rev. Lett. **94**, 187204 (2005).

5 S. Q. Zhou, K. Poteger, J. Von Borany, R. Grötzschel, W. Skorupa, M. Helm, and J. Fassbender, Phys. Rev. B **77**, 035209 (2008).

6 H. Pan, J. B. Yi, L. Shen, R. Q. Wu, J. H. Yang, J. Y. Lin, Y. P .Feng, J. Ding, L. H. Van, and J. H. Yin, Phys. Rev. Lett. **99**, 127201 (2007).

7 H. Pan, Y. H. Feng, Q. Y. Wu, Z. G. Huang, and J. Y. Lin, Phys. Rev. B **77**, 125211 (2009).

8 S. W. Fan, K. L. Yao, and Z. L. Liu et al. Appl. Phys. Lett. 94, 152506 (2009).

9 X. Y. Peng, and R. Ahujia, Appl. Phys. Lett. **94**, 102504 (2009).

10 L. Shen, R. Q. Wu, H. Pan, G. W. Peng, M. Yang, Z. D. Sha, and Y. P. Feng, Phys. Rev. B **78**, 073306 (2008).

11 B. Gu, N. Bulut, T. Ziman, and S. Makekawa, Phys. Rev. B **79**, 024407 (2009).

12 I. R. Shein, A. N. Enyashin, and A. L. Ivanovskii, Phys. Rev. B **75**, 245404 (2007).

13 K. S. Yang, Y. Dai, B. B. Huang, and M. –H. Whangbo, Appl. Phys. Lett. **93**, 132507 (2008).

14 G. Kresse, J. Hafner, Phys. Rev. B **47**, 558 (1994).

15 G. Kresse, J. Furtherműller, Phys. Rev. B **54**, 11169 (1996).

16 J. P. Perdew, K. Burk, M. Ernzerhof, Phys. Rev. Lett. **77**, 3865 (1996).

17 J. P. Perdew, Y. Wang, Phys. Rev. B **45**, 13244 (1992).

18 H. J. Monkhorst, J. D. Pack, Phys. Rev. B **13**, 5188 (1976).

19 N.K. Abrikosov, V.B. Bankina, L.V. Poretskaya, L.E. Shelimova and E.V. Skudnova, Semiconducting II–VI, IV–IV and V–VI Compounds, Plenum, New York (1969).

20 S. B. Zhang and John E. Northrup, Phys. Rev. Lett. 67, 2339 (1991).

21 *CRC Handbook of Chemistry and Physics* 87th ed.; Lide, D. R.Taylor & Francis: London, 2006.

22 S. A. Wolf, D. D. Awschalom, R. A. Buhrman, J. M. Daughton, S. von Molnar, M. L. Roukes, A. Y. Chtchelkanova, and D. M. Treger, Science **294**, 1488 (2001).

23 C. Zener, Phys. Rev. 82, 403 (1951).

24 P. –G. de Gennes, Phys. Rev. 118, 141 (1960).

25 K. A. Kiloin and V. N. Fleurov, Transition Metal Impurities in Semiconductors (World Scientific, Singapore, 1994).

26 A. Zunger, in Solid State Physics, edited by H. Ehrenreich and D. Turnbull (Academic, Orlando, 1986), Vol. 39, p. 276.

TABLE 1. Optimized X-Zn (X= Be, B, C, N) bond lengths. **Total energy difference between** spin polarized (E_{sp}) and non-spin polarized (E_{nsp}) states, $\Delta E = E_{nsp}-E_{sp}$. Formation energy ($E_{form}$) for the introduction of a dopant atom into the S site of ZnS based on the stable configuration. Magnetic moment of X ion M_X, and total magnetization of the supercell, M_{tot}, in its stable state.

Models	X-Zn(Å)	ΔE(meV)	E_{form}(eV)	$M_X(\mu_B)$	$M_{tot}(\mu_B)$
Be@S	2.354	187	**5.47**	0.57	2.00
B@S	2.209	501	**2.69**	1.01	3.16
C@S	2.056	98	**1.49**	0.70	2.38
N@S	1.980	0	**1.33**	0	0

TABLE 2. Be-doped ZnS. Energy difference between FM and AFM spin-ordering ΔE= E(FM)-E(AFM)**. Formation energy (E_{form}) for the introduction of two dopant atoms into the S sites of ZnS based on the stable configuration (FM or AFM)**. **Absolute value of magnetic moment on each Be ion** M_{Be}, and total magnetization of the supercell, M_{tot}, in its stable state (FM or AFM) for different Be-Be distances in the doping configurations shown in Figure 1, *i.e.*, Be(0,i) (i = 1~5).

(0, i)	Be-Be(Å)	ΔE(meV)	$\mathbf{E_{form}}$	$M_{Be}(\mu_B)$	$M_{tot}(\mu_B)$
(0, 1)	3.819	18	**9.00**	**0.20**	0
(0, 2)	5.401	-212	**10.71**	**0.57**	4.10
(0, 3)	6.615	94	**10.52**	**0.56**	0
(0, 4)	7.638	3	**10.27**	**0.001**	0
(0, 5)	9.355	-380	**10.87**	**0.58**	3.98

TABLE 3. B-doped ZnS. Energy difference between FM and AFM spin-ordering ΔE= E(FM)-E(AFM)**. Formation energy (E_{form}) for the introduction of two dopant atoms into the S sites of ZnS based on the stable configuration (FM or AFM). Absolute value of magnetic moment on each B ion** M_B, and total magnetization of the supercell, M_{tot}, in its stable state (FM or AFM) for different B-B distances in the doping configurations shown in Figure 1, *i.e.*, B(0,i) (i = 1~5).

(0, i)	B-B(Å)	ΔE(meV)	E_{form}	$M_B(\mu_B)$	$M_{tot}(\mu_B)$
(0, 1)	3.819	9	**4.81**	**0.74**	0
(0, 2)	5.401	-10	**5.36**	**1.00**	6.36
(0, 3)	6.616	87	**5.30**	**0.97**	0
(0, 4)	7.638	-77	**5.48**	**1.00**	6.27
(0, 5)	9.355	-751	**5.38**	**1.01**	6.30

TABLE 4. C-doped ZnS. Energy difference between FM and AFM spin-ordering ΔE= E(FM)-E(AFM). **Formation energy (E_{form}) for the introduction of two dopant atoms into the S sites of ZnS based on the stable configuration (FM or AFM). Absolute value of magnetic moment on each C ion** M_C, and total magnetization of the supercell, M_{tot}, in its stable state (FM or AFM) for different C-C distances in the doping configurations shown in Figure 1, *i.e.*, C(0,i) (i = 1~5).

(0, i)	C-C(Å)	ΔE(meV)	E_{form}	$M_C(\mu_B)$	$M_{tot}(\mu_B)$
(0, 1)	3.819	56	**2.59**	**0.51**	0
(0, 2)	5.401	4	**2.90**	**0.71**	0
(0, 3)	6.616	-59	**2.68**	**0.83**	4.63
(0, 4)	7.638	-121	**2.67**	**0.67**	3.83
(0, 5)	9.355	0	**2.81**	0	0

Figure 1. 64-atom (2 × 2 × 2) supercell of ZnS employed to define model Be, B, C, and N-doped ZnS structures. The small yellow and large gray spheres represent the S and Zn atoms, respectively. The positions of S substituted by dopant atoms are denoted by 0~5.

Figure 2. (a) Density of states (DOS) and (b) projected density of states (PDOS). Black, red, green, and dark yellow lines represent the total DOS, **dopants** 2p **(2s orbital for Be)**, S 3p, and Zn 3d orbitals, respectively. The dashed line represents the Fermi level E_F.

Figure 3. Spin density for (a) single-C doping (left panel) and (b) two-C doping (right hand) for a FM state separated by 7.638 Å. The yellow isosurface corresponds to the spin-up density.

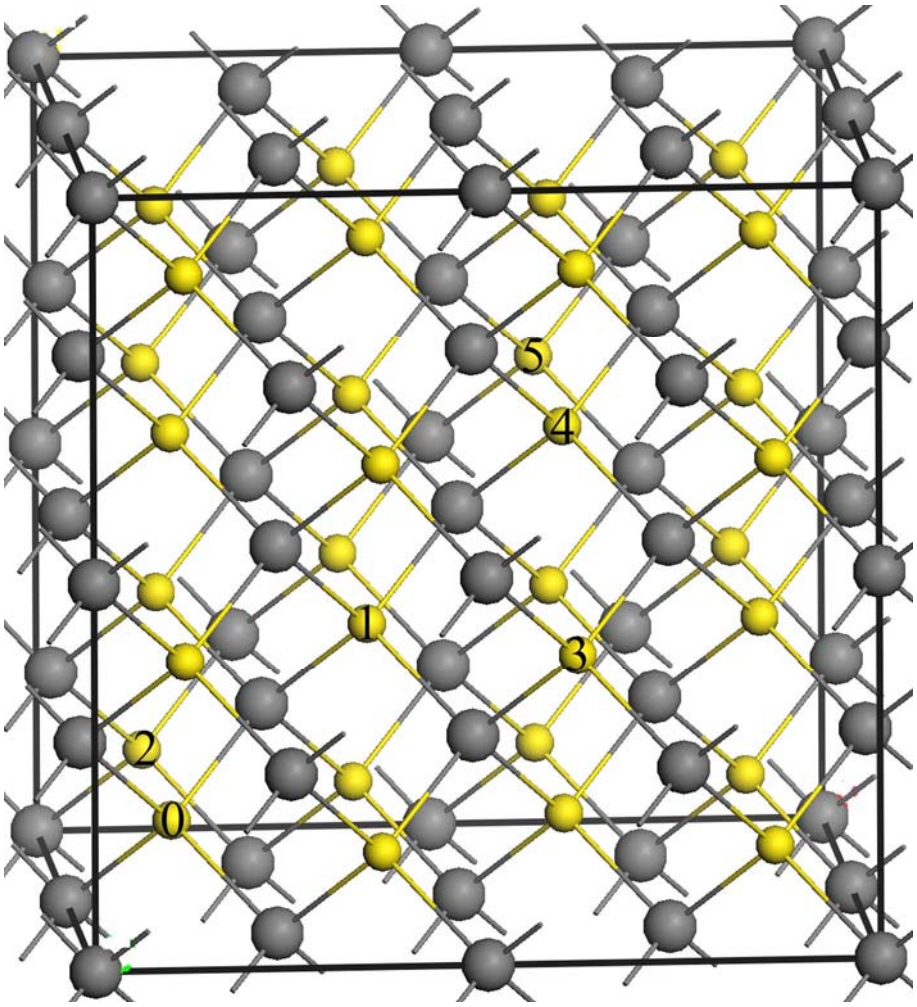

Figure1

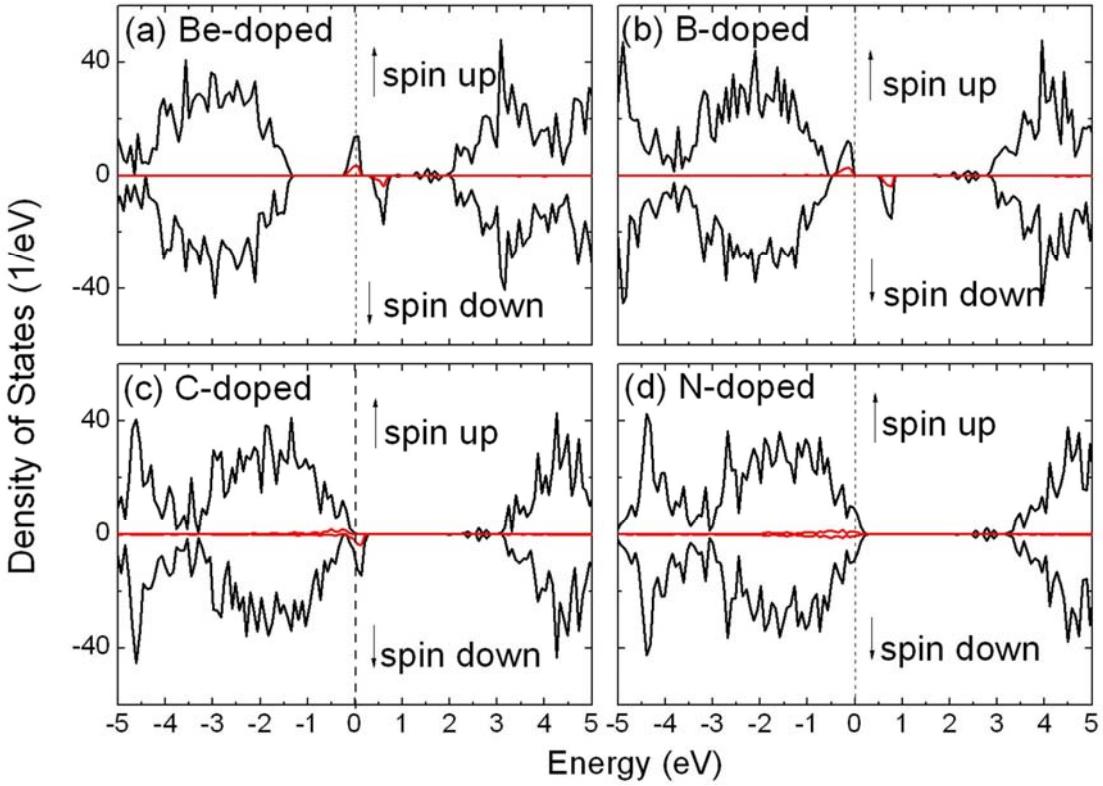

Figure 2 a

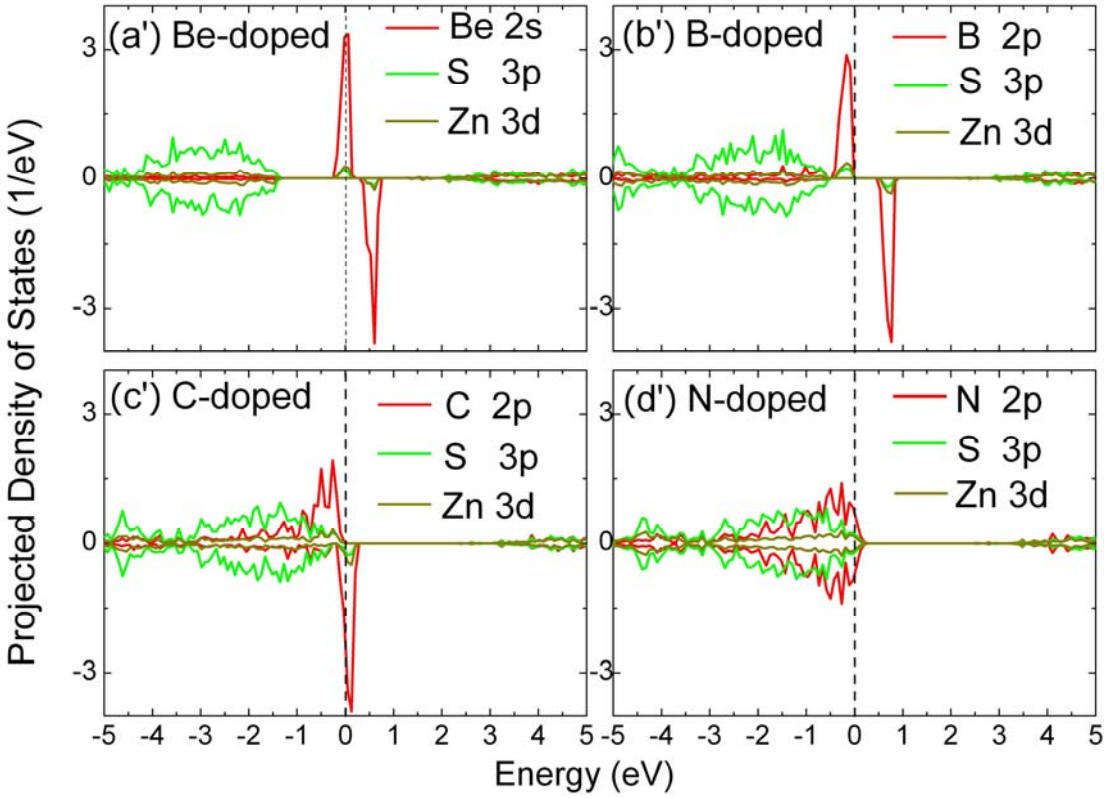

Figure 2b

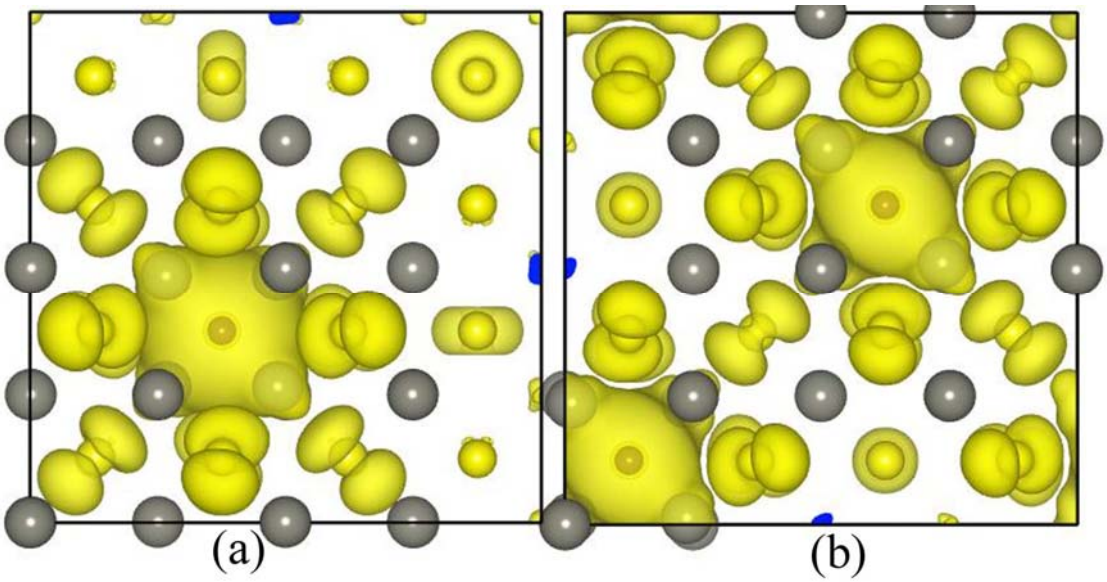

Figure 3